2022 IEEE/ASME International Conference on
Advanced Intelligent Mechatronics (AIM)

2022 IEEE/ASME International Conference on Advanced Intelligent Mechatronics (AIM) | 978-1-6654-1308-4/22/$31.00 ©2022 IEEE | DOI: 10.1109/AIM52237.2022.9863410

A Rigid and Flexible Structures Coupled Underactuated Hand

Qi Liu, Jun Zhang, Xinyi Li, Jingsong Zhou, Xuhui Hu, Weiming Jin, and Aiguo Song

***Abstract*—Robotic hand has vast application potential in home-serviced, medical care, surgery, maintenance, Etc. Various robotic hands made of rigid and flexible materials have been developed in the past decade. In this work, we present a rigid-flexible coupled underactuated hand with good agility and compliance for various kinds of grasping and safe operations. First, the dynamic simulation for finger bending and underactuated hand grasping was studied. Then, a prototype of the underactuated hand was fabricated. Next, we carried out a series of experiments based on the prototype. Single finger bending performance and blocking force were tested, respectively. We also tested the adaptive grasping ability of the hand. Finally, we performed collision experiments and compared the impact forces of the Be Bionic hand and our underactuated hand. Results showed that the underactuated hand could grasp objects with different shapes and possessed a higher degree of safety, reducing impact force by 30% to 50%.**

I. Introduction

With more than 20 degrees of freedom, our hand allows us to perform various activities in daily life. However, accidents and neurological diseases cause many people's hands to lose function every year worldwide. Robotic hand-design service hand movement is a feasible solution. With the help of robotic hands, patients can independently complete many normal activities of daily living like drinking water and getting dressed. In the face of the huge application potential of the robotic hand, various robotic hand design methods have been developed and used in in-home services [1-2], medical care and surgery [3-5], maintenance, and construction activities in the space station [6-7], etc.

Robotic hand manufacturing has a long history, and the earliest records can be traced back to ancient Egypt [8]. The development of traditional rigid robotic hands that adopt rigid parts and structures in design has been very mature. The multi-fingered hand developed by Kaneko et al. has rigid links, harmonic drive gears, and servomotors [9]. The Robonaut Hand [6] is a 14-degrees of freedom robotic hand utilizing a 7-bar linkage and leadscrew mechanisms to realize the finger grasping. The UB hand I, II, III, and IV are four generations of robotic hands developed at the University of Bologna [7, 10-11]. These hands consist of rigid parts connected by ball bearing revolute pairs or elastic hinges and are actuated by tendons and pulleys with electrical motors. DLR and HIT developed several generations of robotic hands focusing on the mechanisms and multisensory investigations [12-14]. The finger motion drive of the hands uses flat brushless DC motors, harmonic drivers, and high-speed timing belts [15]. Kawasaki et al. developed the Gifu Hand II and Gifu Hand III dexterous robot hands, which have planar four-bar linkage mechanisms, reduction gears, and worm gears for the fingers [16-17]. Takaki et al. proposed a force-magnification mechanism consisting of an eccentric cam, a bearing, and a pulley to improve the grasping force of a robot hand [18]. Although the rigid structure has the advantages of mature design and high stability and control accuracy, the rigid structure often makes the robot hand have high weight and volume. At the same time, the lack of flexibility makes the robot hand has the potential of damage in a collision with the environment.

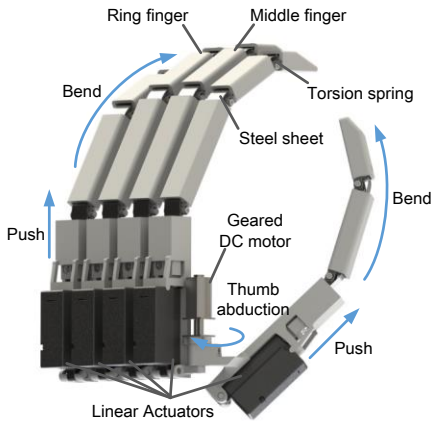

Fig. 1. CAD model of the underactuated hand with six degrees of freedom.

Flexible materials are also increasingly being used to design robotic hands. These materials make the robotic hand possess high flexibility and improve the safety of contact with objects. Among those methods, using fluid to drive the robot hand-made using flexible materials is common. Devi et al. [19] studied the flexible pneumatic actuators driven bending joints of suitable rubber for an under-actuated robotic hand. Li et al. [20] developed FEA, which is actuated by the fluid displaced from tube twisting used in soft finger design. Zhou et al. [21] presented a dexterous soft robotic hand, BCL-13, with 13 independently actuated joints powered by air pressure. In addition to the fluid drive method, scholars have also launched many types of research on the potential of variable material using robot hand design. Wang et al. [22] proposed a soft robotic hand using a layer jamming structure. Lee et al. [23] developed an origami twisted tower-inspired under-actuated robotic gripper. Cho et al. [24] presented a lightweight robotic hand with 16 DOFs using an SMA actuator array. Kim et al. [25] used SMA and woven type smart soft composite to develop a prototype soft robotic hand. The flexible robot hand has the advantages of being soft and lightweight, but its

*This work was supported in part by the National Key R&D Program of China under Grant 2018AAA0103004, National Natural Science Foundation of China under Grants 61873066 and 62173090, and Zhi Shan Scholars Program of Southeast University under Grant 2242020R40096.

The authors are with the State Key Laboratory of Bioelectronics, School of Instrument Science and Engineering, Southeast University, Nanjing 210096, China (e-mail: j.zhang@seu.edu.cn).

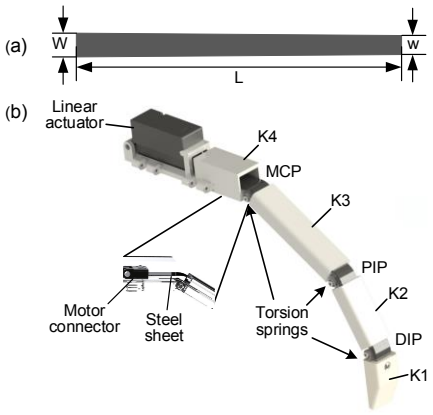

Fig. 2. Rigid-flexible design method for the robotic finger. (a). Parameters of the flexible thin-wall spring steel sheet (FSSS). (b). Rigid-flexible coupled structure design principle which uses FSSS to drive the finger.

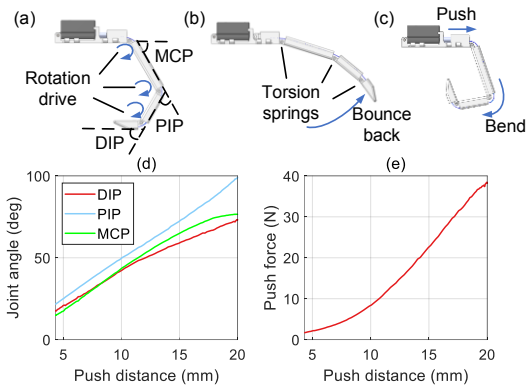

Fig. 3. Simulation steps and results. (a) Add rotational drive to rotate MCP, DIP, and PIP joints. (b) Remove the drive and add torsion springs. (c). The linear actuator pushes forward to its maximum stroke. (d)-(e). Simulation results of the index finger.

driving mechanism is often complex and bulky, which is challenging to realize people's daily portable use.

With the rigid exoskeleton and flexible muscle, the crab leg possesses the advantages of compact structures and powerful protection from outer impacts and injury, which provides a new idea for legged robot design in our previous work [26]. As shown in Fig. 1, this paper presents a rigid and flexible structure coupled underactuated hand with good agility and compliance for various kinds of grasping and safe operations. The mechanisms design, rigid-flexible coupled simulations, and experiments are detailed in the following sections.

II. Compliant Underactuated Hand Design

In this section, we first design the mechanism of one finger of the robotic hand. Then, a six degrees of freedom compliant underactuated hand is designed with five rigid-flexible structures coupled fingers.

A. Rigid-Flexible Structures Coupled Finger Design

Crab legs have a unique structure consisting of the rigid outer exoskeleton and inner flexible muscle. This leg structure enables crabs to traverse uneven terrain agilely and safely. Inspired by the crab leg, a new kind of rigid-flexible structure coupled under-actuated robotic finger is proposed for compliant and safe interaction with the environment. The basic principle of the finger is the coupling movement of rigid parts and flexible structures.

As illustrated in Fig. 2 (b), rigid shells, a flexible thin-wall spring steel sheet (FSSS), and a linear actuator form the robot finger. The rigid shells consist of four finger knuckles, K1 to K4, which connect in series through revolute joints. The length of K1 to K3 is similar to the human finger. Revolute joints between those knuckles become the metacarpophalangeal (MCP), proximal interphalangeal (PIP), and distal interphalangeal (DIP) of the robot finger. Left-hand and right-hand torsion springs are set at the joints with their two legs installed on the adjacent knuckles. FSSS served as the flexible part of the robot finger, mimicking the muscle inside the hard exoskeleton of crab legs to drive its motion. Fig. 2 (a) shows the shape of the FSSS. The FSSS has a trapezoid shape, housing in the narrow slots on K2 and K3. The rear end of FSSS connects with the linear actuator shaft through a motor connector, while the front end of FSSS is fixed at K1. A linear motor and motor connector are hidden in K4.

The FSSS has the rigidity for force transmission and the flexibility for bending under a pushing force. The FSSS will bend with large deformation when one end is fixed while the other is pushed. The FSSS straightens again from bending when the moving end is pulled backward. Under the thrust at its rear end, the FSSS slides in knuckles K2 and K3 and contacts with them. Then, the joints among the MCP, PIP, and DIP joints bend, and the three rotational motions are achieved by the translational motion to realize an under-actuation robotic finger. The rigid shell and FSSS coupling design strategy can effectively limit the local bending of the FSSS and make it bend in a limited range. At the same time, the rigid outer shell provides contact force for the FSSS, making the internal structure of the mechanism more compact and more robust. Those merits enable the finger to bend and stretch when actuated by just the single motor, realizing a very compact structure of the robot finger.

B. Mechanism Design of Compliant Underactuated Hand

Based on the concept of the rigid and flexible structures coupled robotic finger, we design the underactuated hand. The CAD model of the hand is illustrated in Fig. 1. The K4 part of the index, middle, ring, and little fingers are combined to constitute the palm. The linear actuators of the fingers are mounted on the back of the palm. The thumb is connected to the palm through a geared DC motor. All fingers adopt a similar structure design, and the length of each finger is similar to the finger of a human hand. In the robot hand movement, fingers are driven independently by the linear actuators, and the geared DC motor rotates forward and reverses to realize the inward and outward movements of the thumb.

III. Rigid-Flexible Coupled Simulation

To verify the feasibility of the hand design method, we conduct the rigid-flexible coupled simulations of the single finger and the grasping motion of the hand.

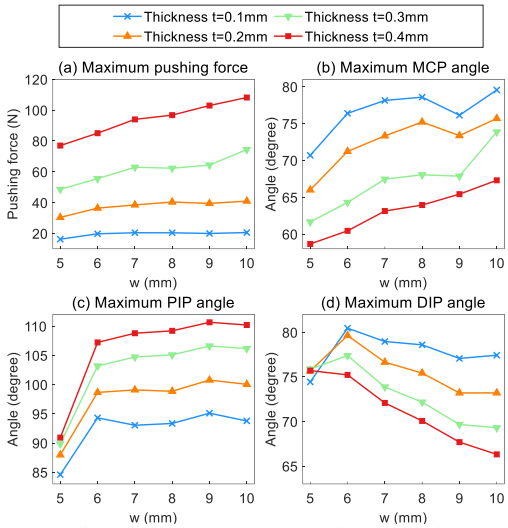

Fig. 4. Bending simulation results of the finger with different shapes. (a) The maximum pushing force. (b)-(d) Rotational angles of MCP, PIP, and DIP.

A. *Single Finger Bending Simulation*

Before evaluating the performance of the whole hand, we use the software of Recurdyn to simulate the motion of the robotic finger through rigid-flexible coupled dynamic simulation. The simulation is divided into three steps, as illustrated in Fig. 3. In the first step, the mechanical finger structure is assembled, and the three joints of the finger are slowly bent to the initial angle of the torsion springs of 120°. Then torsion springs are installed on each joint in the second step while removing all joint rotational drive so that the joints rebound naturally. In the third step, the displacement boundary condition is applied to the connector gently to simulate the linear actuator driving the entire finger to bend. In order to make the simulation more natural, we set nylon as the material of the rigid knuckles and 65Mn as the material of FSSS. The mesh's average size, minimum size, and thickness in the FSSS are set as 2 mm, 0.1 mm, and 0.10 mm to 0.25 mm, respectively, using a Pshell element with a 4-sided quad shell. Fig. 3(d) shows the simulation results of a single finger with the FSSS parameters L=142 mm, w=6 mm, W=10 mm, and t=0.15 mm.

In the bending process, the shape of FSSS will affect the bending performance of the rigid-flexible coupled fingers. Here we try to optimize the shape of FSSS through rigid-flexible coupled dynamic simulation. As shown in Fig. 2(a), Four parameters form the FSSS: bottom width W, top width w, length L, and thickness t. When the length L is fixed, the width W and w affect the gradient of FSSS, and thickness t is closely related to the ease of bending for FSSS. Take the index finger as an example. Under the condition of L=140 mm and W=10 mm, the rigid-flexible coupled dynamic simulations of different top widths w and FSSS thickness are carried out, respectively. After simulation, we extract the thrust required at the finger end and the bending angle of each joint. The results are shown in Fig. 4. We found that the larger the FSSS gradient, the smaller the bending angle of the DIP joint, while the bending angles of the MCP and PIP joint increased gradually.

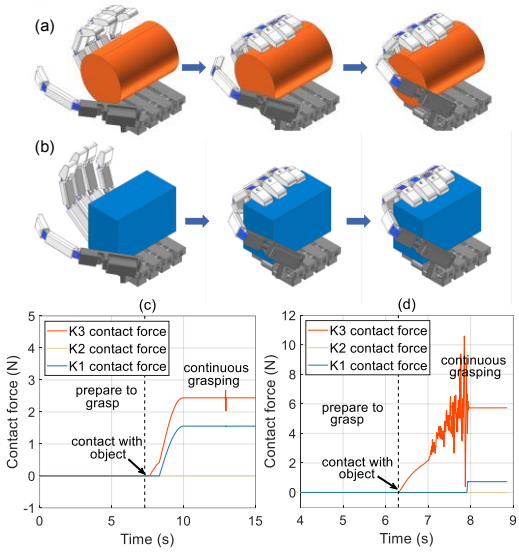

Fig. 5. The underactuated hand adaptively grasps a cylinder and a cube. (a)-(b) Simulation of underactuated hand grasping cylinder and cube showing three states: preparing to grasp, object contact, and continuous grasping. (c)-(d) Contact forces between K1, K2, and K3 of the middle finger and the objects during grasping.

The simulation results indicate that the simple design of the finger can realize bending angle range like a real finger. The pushing force is not very large. By selecting the proper shape parameters of the FSSS, we can design fingers with different bending capabilities for an underactuated hand. The results also can be used to select the proper actuators for the hand prototype. We determine the top width w=6 mm through simulation, thickness t=0.15 mm. In the case of a similar length of 4 fingers, their parameters are similarly designed.

B. *Grasping Simulation of the underactuated Hand*

Based on the single finger bending simulation, we simulate the whole hand grasping process of the rigid-flexible structures coupled underactuated hand.

In the grasping simulation, all degrees of freedom of fingers are driven, including the thumb opposition movement, to grasp a fixed, rigid body. Three steps of rigid-flexible underactuated hand grasping an object are observed in the simulation: preparatory, contact, and continuous grasp. At the preparatory step, the fingers of the hand gradually bend to prepare for contact with the object using a specific grasping gesture. The fingertip or finger abdomen contacts and fixes the object in the contact phase. In the continuous grasping stage, due to the flexibility of the finger structure, the finger automatically adapts to the shape of the rigid object.

Two different shapes of objects are used in the grasping simulation: cylinder and cube. Fig. 5 (a) and (b) show the three steps of the rigid-flexible coupled dynamic simulation of the hand grasping those two objects. In case of slip-off, objects are fixed in a position convenient for the underactuated hand to grasp. In the simulation process, manual adjustments are taken on the motion drive to help the underactuated hand complete the grasping action. Fig. 5 (c) and (d) show the contact force between three knuckles of the middle finger and the grasping objects. The results show that the contact force increases

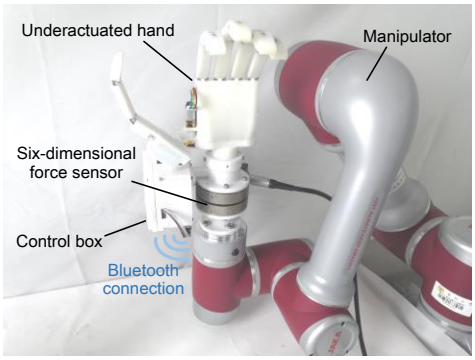

Fig. 6. Prototype of rigid-flexible coupled underactuated hand mounting on a manipulator for experiments.

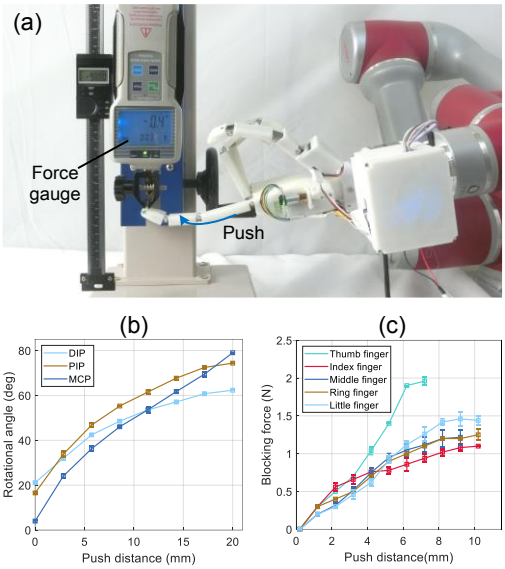

Fig. 7. Finger motion performance and blocking force test results. (a) Single finger experiment scene. (b) Finger motion performance shows the bending angle of each joint of the index finger. (c) Blocking force at the fingertip of each finger when force gauge pushing.

during the object contact stage and keeps nearly constant in the continuous grasping stage. However, there is a large fluctuation in the cube grasping, which is caused by the discontinuous surface of the cube. Because the grasping object is fixed in the simulation, the K2 contact force is always 0 N. This phenomenon can be improved by releasing the freedom of movement of the grasping object.

IV. Prototype Fabrication And Experiments

Based on the mechanism design and rigid-flexible coupled simulations of the compliant finger and under-actuated hand, a prototypical underactuated hand was fabricated for experimental studies.

A. Underactuated Hand Prototype and Experimental Setup

Fig. 6 shows the designed hand prototype. The K4 knuckles of the index, middle, ring, and little fingers constitute the palm of the robot hand. The linear actuators are installed on the back of the palm. The control box mounted on the wrist of the hand houses a control unit and a 500mAh battery. The knuckles and control box were 3D printed using nylon with a

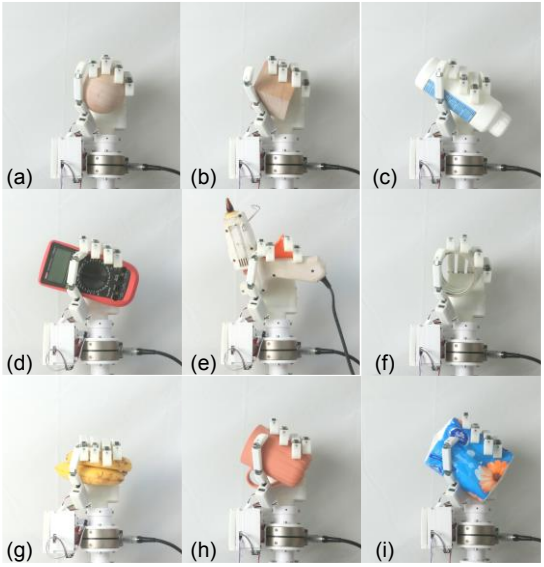

Fig. 8. Adaptive grasping movement experiments (a) Wooden ball. (b) Wooden square. (c) Plastic bottle with liquid. (d) Multimeter. (e) Glue gun. (f) Tape. (g) Banana. (h) Cup. (i) Paper extraction.

density of 1.15 g/cm^3 and a bending strength of 72 Mpa. The 65Mn was used to fabricate the FSSS with different lengths. Other size parameters of the FSSS used in the fingers were t=0.15 mm, w=6 mm, and W=10 mm. The PQ12-R linear actuators from Actuonix were used to drive the robot finger, providing up to 45 N thrust with a range of 20 mm and a maximum thrust speed of 15 mm/s. The gear motor N20 with encoder was chosen to drive the thumb for inward and outward movements. The maximum torque of the N20 motor can reach 0.29 N·m with a rated speed of 34 rpm. The control unit with the STM32RCT6 MCU controls the movement of the hand and receives the current of the actuators for safe control. The control unit also can communicate with a laptop through Bluetooth. The hand is about 20 cm long and 580 g in weight, including all the mechanical parts and electronics.

As shown in Fig. 6, an experimental setup was also built to facilitate the hand performance tests. The wrist of the hand is mounted on the six-dimensional force sensor which is connected to the 6 degrees of freedom manipulator JAKA Zu 7. The manipulator drives the hand to move in a limited 3D space for object grasping and other operations. In addition, the force sensor can measure the force received at the end of the hand during the interaction with the environment for safe motion control and estimating the compliance of the hand.

B. Single Finger Bending Performance and Blocking Force

The performance of the robot finger determines the function of the underactuated hand. Here we first used a single finger to conduct the experiments of finger bending and blocking force.

Taking the index finger as an example, we fixed the underactuated hand on the manipulator in the bending performance experiment. Then, we controlled the linear actuator to move from 0 mm to 20 mm ten times at a constant speed, pushing the index finger to bend and stretch. A camera recorded this process with 30 fps and 1920×1080 pixels. The

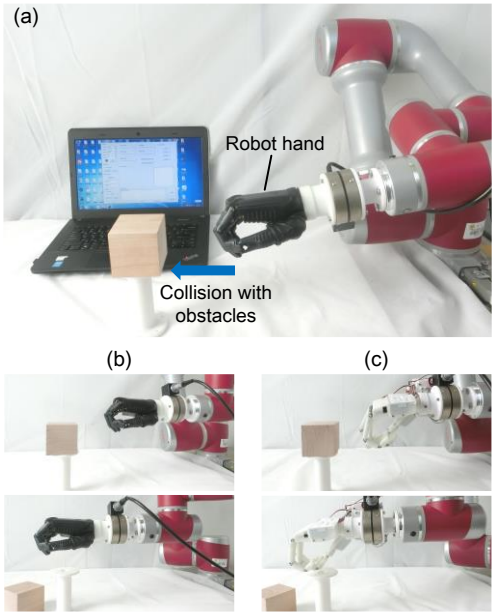

Fig. 9. Experiment scenario of collision safety tests. (a) The procedure of collision experiment showing with the BeBionic hand. (b) Motion trajectory of the BeBionic hand. (c) Motion trajectory of our underactuated hand.

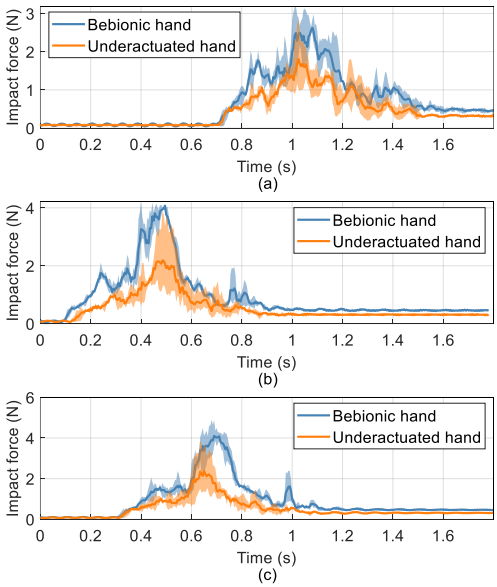

Fig. 10. Impact force experiment results. (a) The impact force of bebionic hand and underactuated hand at the speed of 2 m/s. The average maximum impact is 2.63 N of the bebionic hand and 1.81 N of the dexterous hand. (b) The impact force of the bebionic and underactuated hand at the speed of 2.25 m/s. The average maximum impact is 4.08 N of the bebionic and 2.18 N of the dexterous hand. (c) The impact force of bebionic hand and underactuated hand at the speed of 2.5 m/s. The average maximum impact is 4.10 N of the bebionic hand and 2.38 N of the dexterous hand.

Tracker software processed the video, and the calculated bending angle of each joint is drawn in Fig. 7 (b). The average maximum bending angles of MCP, PIP, and DIP are 82.8º, 74.2º, and 64.5º, respectively. The results show that the proximal joint is more accessible to turn than the finger joint far from the actuator, which is different from the simulation results represented in the finger simulation. This discrepancy may be caused by the large-area contact friction between the FSSS and knuckles.

At the same time, we tested the blocking force of the finger using the experimental platform shown in Fig. 7(a). The robot hand was mounted on the manipulator's end, and the index fingertip was in contact with a force gauge. The linear actuator continuously drove the finger to bend and push the gauge during the experiment until the force value was stable. Among the pressure gauge used in the test is ZP-500, which measurement range can reach 500 N with an accuracy of 0.1 N. Fig. 7(c) shows the experimental results. Different fingers are tested five times, and the maximum thrust of the five fingers can reach: 1.96 N, 1.1 N, 1.25 N, 1.2 N, and 1.44 N, respectively. The results show that fingers with fewer or shorter joints tend to have higher blocking force.

C. *Underactuated hand Adaptive Grasping*

In this section, we tested the human hand gesture imitation and grasping ability of the robotic hand. Objects in activities of daily life come in a wide variety of shapes. In this experiment, the robotic hand was tested with common gestures of human grasp and the objects used in daily life. As we tested, the hand can mimic many human hand grasp gestures.

When objects are placed in an appropriate position for the robot hand to grasp, according to the different lengths of each finger, instructions are sent to the linear actuators and control the hand to grasp with different grasping gestures defined in [27]. We controlled the hand to grasp objects of different shapes and sizes. In these tests, the robotic hand successfully grasped more than 10 kinds of objects used in daily life like tape, sponge block, screwdriver, etc. The grasping results of the hand are shown in Fig. 8. Fig. 8(a) to (c) shows the robot hand grasping objects of regular shape: sphere, square, and cylinder. Fig 8(d) to (f) show that the robot hand grasps tools used in daily life with a higher degree of shape irregularity: multimeter, glue gun, and tape. We also measured the grasping performance of daily life objects like bananas, cups, and paper extraction shown in Fig. 8(g) to (i). The results indicate that the hand can mimic a great number of human hand grasp gestures and grasp various objects compliantly and safely.

D. *Robot Hand Collision Experiment*

Safety is essential to an underactuated hand and the object it operates, determining the possibility of damage in use. Therefore, we designed a non-destructive collision experiment to test the performance of our underactuated hand and compare its characteristics with the commercial BeBionic hand from Ottobock.

In the experiments, our underactuated hand and the BeBionic hand were mounted on the end of the manipulator. The six-dimensional force sensor connected between the hand and the manipulator recorded the force when the hand collided with an object. A wooden cube with the size of 7 cm×7 cm×7 cm was freely placed on a 3D printed cylindrical part which was fixed on the desk, as shown in Fig. 9(a). In the

manipulator coordinate system, the hands moved uniformly from the initial position (170.1 mm, −228.5 mm, 215 mm) to (170.1 mm, −358.9 mm, 215 mm). Fig. 9(b) and (c) illustrate the trajectories of the two hands.

In the movement process, the hands collided with the wooden cube at speeds of 2 m/s, 2.25 m/s, and 2.5 m/s, respectively. The wooden cube dropped on the table during the collision. The tests were performed three times at each speed. The force sensor measured the end force applied on the twist of the hands in the collision process. The force changes are shown in Fig. 10(a)-(c). The results show that the impact force between the hands and the rigid wooden cube increases when the collision velocity increases, showing a growing potential safety hazard. However, compared with the BeBionic hand, the underactuated hand can reduce the maximum impact force by 30% to 50% due to its compliance, proving that the rigid-flexible coupled structure has a higher level of safety.

V. Conclusions And Future Work

This paper designs an adaptive underactuated hand with a rigid-flexible coupled structure. The structure transforms the linear actuator motion into the rotation of three joints in one finger. This design makes the underactuated hand more compact and can be easily controlled. In this paper, we carried out a single finger bending simulation and optimized the shape of the FSSS. The underactuated hand grasping simulation was also studied. Then, a prototype was made and tested. Finger bending and blocking force were tested to verify the feasibility of the design method. Then we controlled the underactuated hand to grasp objects with different shapes. Furthermore, we carried out the collision experiment on the hand and compared it with the Bebionic hand. The results showed that the underactuated hand could adaptively grasp and possessed a higher degree of safety, reducing the impact force by 30% to 50%.

However, there are still some limitations and more potential for further research. Firstly, the mechanical parts of the hand will be optimized to reduce its mass. Secondly, position and force feedback closed-loop control of the hand will be implemented. Thirdly, we will optimize the design of the thumb to improve the grasping control ability of the hand.

References

[1] W. Chung, C. Rhee, Y. Shim, H. Lee, and S. Park, "Door-Opening control of a service robot using the multifingered robot hand," *IEEE Trans. Ind. Electron.*, vol. 56, no. 10, pp. 3975–3984, 2009.

[2] N. Endo, F. Iida, K. Endo, Y. Mizoguchi, M. Zecca, et al., "Development of the Anthropomorphic Soft Robotic Hand WSH-1R," in: *Proc. First IFToMM Asian Conf. Mech. Mach. Sci. AsianMMS*, Taipei, 2010. pp. 506-512.

[3] H. Liu, M. Selvaggio, P. Ferrentino, R. Moccia, and S. Pirozzi, "The MUSHA Hand II: A Multi-Functional Hand for Robot-Assisted Laparoscopic Surgery," *IEEE/ASME Trans. Mechatronics*, vol. 26, no. 1, pp. 393-404, 2020.

[4] P. Polygerinos, K. C. Galloway, E. Savage, M. Herman, K. O. Donnell, and C. J. Walsh, "Soft robotic glove for hand rehabilitation and task specific training," in: *Proc. IEEE Int. Conf. Robot. Autom.*, Seattle, USA, 2015, pp. 2913–2919.

[5] P. Polygerinos, Z. Wang, K. C. Galloway, R. J. Wood, and C. J. Walsh, "Soft robotic glove for combined assistance and at-home rehabilitation," *Rob. Auton. Syst.*, vol. 73, pp. 135–143, 2015.

[6] C. S. Lovchik and M. A. Diftler, "The Robonaut hand: a dexterous robot hand for space," in: *Proc. IEEE Int. Conf. Robot. Autom.*, Montreal, Canada, 1999. vol. 2, pp. 907–912.

[7] C. Melchiorri, G. Palli, G. Berselli, and G. Vassura, "Development of the UB Hand IV: Overview of Design Solutions and Enabling Technologies," *IEEE Robot. Autom. Mag.*, vol. 20, no. 3, pp. 72–81, 2013.

[8] R. Walkler, "Developments in dexterous hands for advanced robotic applications," in: Proc. *the Sixth Biannual World Autom. Cong.*, Seville, Spain, 2004. pp. 123-128.

[9] K. Kaneko, K. Harada, and F. Kanehiro, "Development of Multi-fingered Hand for Life-size Humanoid Robots," in: *Proc. IEEE Int. Conf. Robot. Autom.*, Roma, Italy, 2007. pp. 913-920.

[10] C. Bonivento, E. Faldella, G. Vassura, "The University of Bologna Robotic Hand Project: current state and future development." In: *IEEE Int Conf. Adv Rob.*, Pisa, Italy, 2002, pp. 349-356.

[11] F. Lotti, P. Tiezzi, G. Vassura, L. Biagiotti, G. Palli, and C. Melchiorri, "Development of UB Hand 3: Early results," in: *Proc. IEEE Int. Conf. Robot. Autom.*, Barcelona, Spain, 2005. pp. 4488–4493.

[12] J. Butterfass, G. Hirzinger, S. Knoch, and H. Liu, "DLR's multisensory articulated hand. I. Hard- and software architecture," in: *Proc. IEEE Int. Conf. Robot. Autom.*, Leuven, Belgium, 1998. vol. 3, pp. 2081-2086.

[13] X. H. Gao, M. H. Jin, J. Li, Z. W. Xie, and G. Hirzinger, "The HIT/DLR dexterous hand: work in progress," in: *Proc. IEEE Int. Conf. Robot. Autom.*, Taipei, Taiwan, 2003. pp. 3692-3697.

[14] L. Hong, P. Meusel, G. Hirzinger, M. Jin, and Z. Xie, "The Modular Multisensory DLR-HIT-Hand: Hardware and Software Architecture," *IEEE/ASME Trans. Mechatronics*, vol. 13, no. 4, pp. 461–469, 2009.

[15] H. Liu, K Wu, P. Meusel, N. Seitz, G. Hirzinger, et al., "Multisensory five-finger dexterous hand: The DLR/HIT Hand II," in: *Proc. IEEE/RSJ Int. Conf. on Intell. Rob. Syst.*, Nice, France, 2008. pp. 3692-3697.

[16] H. Kawasaki, T. Komatsu, and K. Uchiyama, "Dexterous anthropomorphic robot hand with distributed tactile sensor: Gifu hand II," *IEEE/ASME Trans. Mechatronics*, vol. 7, no. 3, pp. 296–303, 1999.

[17] T. Mouri, H. Kawasaki, K. Yoshikawa, J. Takai, and S. Ito, "Anthropomorphic robot hand: Gifu hand III," in: *Proc. of Int. Conf. ICCAS*, Muju, Korea, 2002. pp. 1288-1293.

[18] T. Takaki and T. Omata, "High-Performance Anthropomorphic Robot Hand With Grasping-Force-Magnification Mechanism," *IEEE/ASME Trans. Mechatronics*, vol. 16, no. 3, pp. 583–591, 2011.

[19] Mata Amritanandamayi Devi, G. Udupa, and P. Sreedharan, "A novel underactuated multi-fingered soft robotic hand for prosthetic application," *Rob. Auton. Syst.*, vol. 100, pp. 267–277, 2018.

[20] Y. Li et al., "A dual-mode actuator for soft robotic hand," *IEEE Robot. Autom. Lett.*, vol. 6, no. 2, pp. 1144–1151, 2021.

[21] J. Zhou, J. Yi, X. Chen, Z. Liu, and Z. Wang, "BCL-13: A 13-DOF soft robotic hand for dexterous grasping and in-hand manipulation," *IEEE Robot. Autom. Lett.*, vol. 3, no. 4, pp. 3379–3386, Oct. 2018.

[22] X. Wang, L. Wu, B. Fang, X. Xu, H. Huang, and F. Sun, "Layer jamming ‐ based soft robotic hand with variable stiffness for compliant and effective grasping, " *Cogn. Comput. Syst.*, vol. 2, no. 2, pp. 44 ‐ 49, 2020.

[23] K. Lee, Y. Wang, and C. Zheng, "TWISTER Hand: Underactuated Robotic Gripper Inspired by Origami Twisted Tower," *IEEE Trans. Robot.*, vol. 36, no. 2, pp. 488–500, 2020.

[24] K. J. Cho, J. Rosmarin, and H. Asada, "SBC hand: A lightweight robotic hand with an SMA actuator array implementing C-segmentation," in: *Proc. IEEE Int. Conf. Robot. Autom.*, Roma, Italy, 2007. pp. 921–926.

[25] H.-I. Kim, M.-W. Han, W. Wang, S.-H. Song, H. Rodrigue, et al., "Design and development of bio-mimetic soft robotic hand with shape memory alloy," in: *Proc. IEEE Int. Conf. Robot. Biomim.,* Zhuhai, China, 2015. pp. 2330–2334.

[26] J. Zhang, Q. Liu, J. Zhou, and A. Song, "Crab-inspired compliant leg design method for adaptive locomotion of a multi-legged robot," *Bioinspir. Biomim.*, vol. 17, no. 2, 025001, 2022.

[27] T. Feix, R. Pawlik, H. B. Schmiedmayer, J. Romero, and D. Kragic, "A comprehensive grasp taxonomy," in: *Proc. Fifth RSS Conf. workshop on understanding the human hand for advancing robotic manipulation*, University of Washington, Seattle, USA, 2009. vol. 2, no. 2.3, pp. 2-3.